



Electrochemical Preparation of Porous Copper Surfaces in Zinc Chloride-1-ethyl-3-methyl Imidazolium Chloride Ionic Liquid

Yi-Wen Lin, Chia-Cheng Tai, and I-Wen Sun^{*z}

Department of Chemistry, National Cheng Kung University, Tainan, Taiwan 70101

The preparation of porous copper or copper-zinc surfaces by electrochemical formation of binary Cu–Zn alloys on Cu substrate and subsequent electrochemical etching of the zinc was investigated in a zinc chloride-1-ethyl-3-methylimidazolium chloride ionic liquid at 120°C. Cyclic voltammetry and X-ray diffraction measurements suggested that phase transformation from γ - to β' -Cu–Zn alloy occurred during constant potential dealloying. Essentially all the Zn content in the Cu–Zn could be removed from the alloy with dealloying at a sufficiently positive potential. Dealloyed materials exhibited well-developed bicontinuous porous structure. The dependence of the surface morphology of the porous Cu film on several experimental parameters, including deposition current and charge, and anodizing potential and temperature, were examined.
© 2007 The Electrochemical Society. [DOI: 10.1149/1.2724154] All rights reserved.

Manuscript submitted November 29, 2006; revised manuscript received February 5, 2007. Available electronically April 18, 2007.

Porous copper is an interesting electrode material for the electrolysis process such as hydrogenation of CO₂ into methanol.^{1–3} Porous copper electrodes have been prepared by selective dissolution of aluminum from CuAl₂ alloy in NaOH solutions. This process is known as dealloying and has also been applied for the preparation of other porous metals, and the mechanism for formation of porous metal surfaces by the dealloying process has been well discussed.^{4–12} In brief, the formation of porous structure is a result of a competition between the selective dissolution roughening process of the less noble metal and the surface diffusion smoothing process of the more noble metal. While thermal casting or sputter deposition methods are often employed for the preparation of the precursor alloy CuAl₂, the electrodeposition method was not used because it is difficult to find a suitable electrolyte for the electrodeposition of aluminum. To overcome this, Cu–Zn, which can be formed electrochemically, may be used in place of CuAl₂.

Zinc chloride reacts with 1-ethyl-3-methylimidazolium chloride (ZnCl₂-EMIC), forming ionic liquids that are liquids near or below ambient temperature.¹³ This ionic liquid system has been investigated for electrodeposition applications.^{14–16} ZnCl₂-EMIC is an aprotic medium and provides a wide working temperature covering from room temperature to above 150°C. The high working temperature may be advantageous for electrodeposition of alloys. Recently, the fabrication of nanostructured platinum, gold, and silver films on the surface of corresponding electrodes by electrochemical alloying/dealloying in the ZnCl₂-EMIC without using hazardous acids or bases has been demonstrated.^{17–19} This method provides an easy way to form porous metal films, and because the zinc(II) species that was consumed during the electrodeposition step was redissolved into the ZnCl₂-EMIC ionic liquid during the electrochemical dealloying step, the ZnCl₂-EMIC ionic liquid is reusable. In previous studies, the effects of the experimental factors such as deposition current, potential, and temperature on the structure of the porous metal films have been examined. To verify the previous findings and further explore this electrochemical alloying/dealloying approach, this present paper examines the fabrication of porous copper films by electrochemical formation and electrochemical dealloying of Cu–Zn alloys in a 50–50 mol % ZnCl₂-EMIC ionic liquid. The Cu–Zn alloy phase change during the anodic dealloying step is noticed.

Experimental

Synthesis of ZnCl₂-EMIC ionic liquid.—EMIC was prepared and purified according to the method described in literature.²⁰ The ZnCl₂-EMIC ionic liquid was prepared in a Vacuum Atmospheres

glove box filled with dry nitrogen by mixing proper amounts of ZnCl₂ (98% Aldrich) and EMIC at 90°C for 6 h. The resulting ionic liquid was colorless.

Fabrication of porous copper surface.—The fabrication of porous copper was conducted in a dry nitrogen-filled glove box. The electrochemical experiments were accomplished with an Autolab potentiostat/galvanostat controlled with GPES software. A three-electrode electrochemical cell was used for the electrochemical experiments. The reference electrode was a Zn wire (Aldrich, 99.99%) placed in separated fritted glass tube containing pure 50–50 mol % ZnCl₂-EMIC ionic liquid. The counter electrode was a Zn spiral immersed in pure 50–50 mol % ZnCl₂-EMIC contained in a fritted glass tube. Preliminary studies showed that similar results were obtained at both Cu plates and Cu wires. The Cu (Aldrich, 99.99%) working electrode was cleaned by immersion in 2 M HNO₃ and rinsed with deionized water (specific resistivity 18.2 M cm) and dried before use. To fabricate the porous Cu electrode, Cu–Zn surface alloys were first formed by electrodeposition of Zn at the Cu wire in a 50.0–50.0 mol % ZnCl₂-EMIC ionic liquid. It was found that the electrodeposition of Zn could be promoted by increasing the temperature. However, if the temperature was too high, the electrodeposits became poorly adhered to the substrate. As a result, the electrodeposition was performed at 120°C in this study. After the electrodeposition, the Zn in the Cu–Zn surface alloys was anodically stripped to create the porous surface. The microstructure of the electrode was examined with a Philips XL40 field emission scanning electron microscope (FESEM). The crystalline phases of the metal samples were examined with a Shimadzu XD-D1 X-ray diffractometer (XRD).

Results and Discussion

Cyclic voltammetry of Zn on Cu substrate.—In order to understand the electrochemical behavior of the Zn(II)/Zn couple and the formation of Cu–Zn alloy in the 50.0–50.0 mol % ZnCl₂-EMIC ionic liquid, cyclic voltammetry was conducted at a polycrystalline Cu wire electrode at 120°C. A typical cyclic voltammogram is shown in Fig. 1. For comparison, a voltammogram for the pure ionic liquid recorded at a glassy carbon electrode (GCE) is also included in this figure. As shown in Fig. 1A, the electrodeposition of Zn at GCEs that occurs at potentials more negative than 0.0 V requires a nucleation overpotential. Figure 1B shows that the electrodeposition of Zn at Cu electrode occurs at a potential more positive than 0.0 V without the nucleation current loop, indicating that the electrodeposition of Zn at Cu may be facilitated by the formation of Cu–Zn alloys. While Fig. 1A shows a single anodic wave for the stripping of the Zn electrodeposits on the GCE, Fig. 1B shows that multiple stripping waves are observed on the Cu electrode, indicating the formation of different surface Cu–Zn alloys by the electrodeposited

* Electrochemical Society Active Member.

^z E-mail: iwsun@mail.ncku.edu.tw

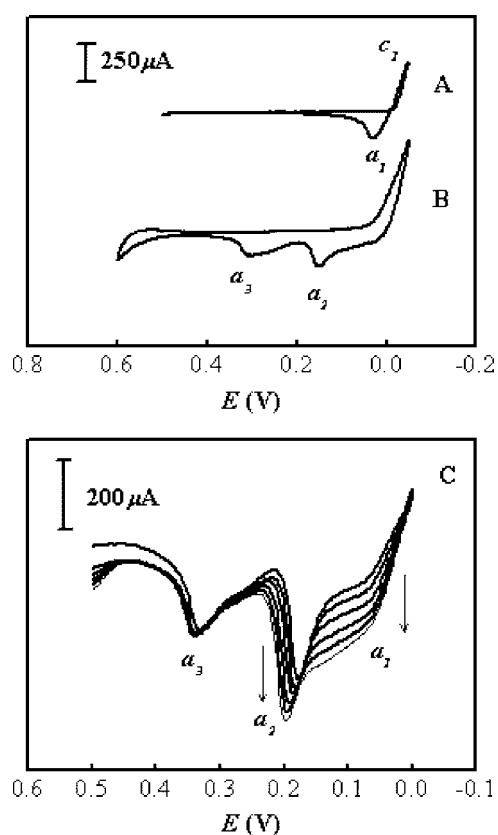


Figure 1. Cyclic voltammograms recorded in a 50.0–50.0 mol % ZnCl_2 -EMIC ionic liquid at: (A) a glassy carbon disk electrode and (B) a copper electrode at 120°C . (C) Stripping voltammograms recorded at a copper electrode after different zinc deposition periods. The scan rate was 50 mV s^{-1} .

Zn and the Cu substrate. According to the phase diagram of the Cu–Zn system,²¹ α -Cu–Zn is stable at 0–30 atom % Zn. β' -CuZn is approximately a 1:1 compound, and γ -CuZn exists at 60–67 atom % Zn. At even higher Zn content, ϵ - and η -CuZn may appear. Figure 1C shows the linear scan stripping voltammograms recorded on the Cu electrode after the constant potential deposition of Zn for different periods of time. This figure shows that when the amount of deposited Zn was increased by increasing the deposition period, waves a_1 and a_2 increased in magnitude whereas wave a_3 approached a limiting value. From these results and the Cu–Zn phase diagram, the broad anodic wave a_1 may be attributed to the dissolution of Zn from alloys such as γ -CuZn that have high Zn content, whereas wave a_2 may be due to the anodic dissolution of Zn from β' -CuZn alloy. Finally, the dissolution of α -Cu–Zn occurs at wave a_3 . Because the anodic stripping of the Zn in the Cu–Zn alloys occurred at potentials far less positive than that for anodizing the Cu substrate, it is possible to fabricate porous Cu through electrochemical etching (dealloying) of the Zn from the Cu–Zn alloy.

Cross-sectional SEM images of the Zn-deposited Cu samples.— Figure 2 shows the typical cross-sectional SEM images and the distribution of Cu and Zn contents in the samples that were obtained by electrodeposition of zinc on copper at 120°C . Figure 2A shows the image of a Cu sample that had been galvanostatically deposited with Zn and was immediately removed from the ionic liquid after the electrodeposition process. On this sample, the deposited Zn layer has a thickness slightly larger than $1\ \mu\text{m}$. The Zn content decreased from the surface toward the inner substrate forming alloy with Cu. Figure 2B shows the image of a sample that had been prepared with the same manner as Fig. 2A, but this sample had been immersed in the ionic liquid at 120°C at open-circuit potential

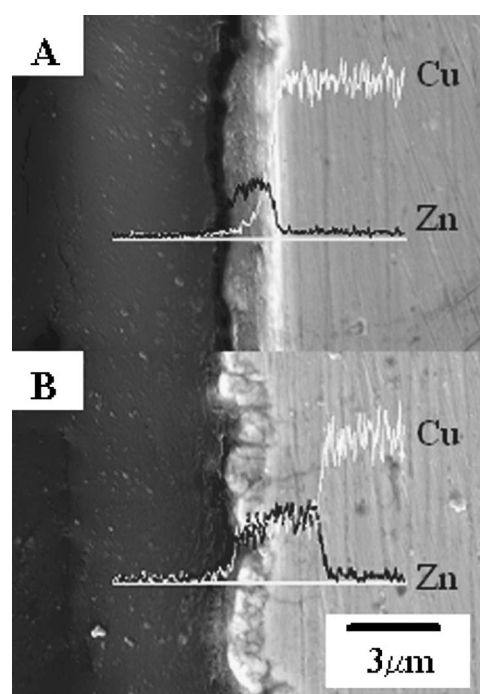


Figure 2. Cross-sectional SEM images and the distribution of Cu and Zn contents in the samples that were obtained by electrodeposition of 2.54 C cm^{-2} Zn on Cu at 120°C . (A) The sample was kept at room temperature after the deposition. (B) The sample had been kept in the ionic liquid at 120°C for 12 h after the deposition.

for 12 h after the conclusion of the electrodeposition. It can be seen that although the initial deposited Zn layer was about $1\ \mu\text{m}$, the Cu–Zn alloy layer has thickened to about $3\ \mu\text{m}$ because of the interdiffusion of Zn and Cu atoms. The fact that Cu also appears in the top $1\ \mu\text{m}$ deposited Zn layer indicates that the alloy layer was formed not only by diffusion of the deposited Zn atoms into the Cu substrate but also by diffusion of Cu atoms to the deposited Zn layer. However, no significant alloy thickening was observed if the Zn-deposited Cu sample was kept at room temperature after the electrodeposition experiment, indicating that the interdiffusion of Zn and Cu atoms was substantially retarded at lower temperature. This result is similar to that observed in the previous study on Ag–Zn systems¹⁹ and confirms that temperature is an important factor on the alloying process. To minimize the variation in the alloy thickness due to the immersion period, in the subsequent experiments, the dealloying step was performed immediately after the deposition step.

XRD measurements.— XRD measurements were conducted to investigate the crystallographic properties of the Zn-deposited Cu samples. Figure 3A shows the results of the as-deposited Cu–Zn sample; this sample exhibits primarily the diffraction patterns of γ -CuZn (or CuZn_2) alloy in addition to those of pure zinc and copper. Figure 3B shows that the diffraction patterns of γ -CuZn have transformed to those of the β' -CuZn (Cu_5Zn_8 and CuZn) alloy after anodic treatment of the as-deposited Cu–Zn sample at 0.10 V . However, patterns of α -Cu–Zn were not observed when the Cu–Zn alloy was anodized at 0.3 V , probably due to the very small amount of this alloy compared to other constituents. When the Cu–Zn alloy samples were anodized at 0.4 V , XRD diffraction patterns like that shown in Fig. 3C were obtained, which indicates that only Cu remained and essentially all the Zn in the surface alloy had been removed. Figure 3D shows the patterns of a Cu–Zn sample that has been immersed in the ionic liquid at 120°C for 12 h after the electrodeposition (the sample similar to that shown in Fig. 2B). This

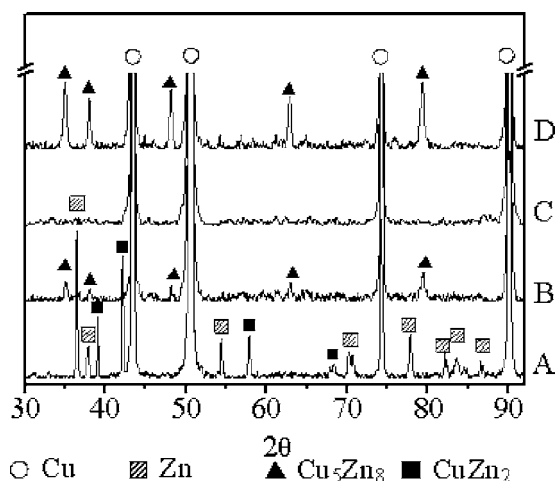


Figure 3. XRD patterns (Cu K α) of Zn-deposited Cu samples from ZnCl₂-EMIC ionic liquid at 120°C: (A) as deposited, (B) after being dealloyed at 0.10 V, (C) after being dealloyed at 0.40 V, and (D) Cu-Zn sample immersed in the ionic liquid for 12 h after the electrodeposition step (i.e., the sample shown in Fig. 2B).

figure indicates that the γ -CuZn has transformed to β' -CuZn. The phase transformation behavior has also been reported during the dealloying of Ni-Zn alloy in a ZnCl₂-NaCl molten salt system.²²

Formation of porous copper.—Porous copper samples were prepared by selective anodic stripping of Zn off the electrochemically formed Cu-Zn alloys. The total dissolution rate of the Zn is affected by the charge-transfer rate (which is determined by the applied anodic potential), the changing in the active surface area for the dissolution, and the mass transport of the metal atoms. Figure 4 shows the typical current vs time curves during constant potential dealloying of the Cu-Zn alloys at 0.40 V at 120°C. This figure shows that the Zn dissolution rate (current) quickly reached a steady-state value until most of the Zn was dealloyed, and then decayed afterwards. The steady-state dealloying current suggests that the rate of the creation of new active sites equals to that of the removal of active dissolution sites. It is worth to mention that the steady-state *i-t* behavior observed in this figure is different from that was observed during the dealloying of Zn from Ag-Zn alloy. For the dealloying of Ag-Zn, the dealloying current increased with time until a maximum value was reached, indicating that the creation of active sites was slow in the early part of the dealloying but increased with time during the dealloying process. The exact reason of such a

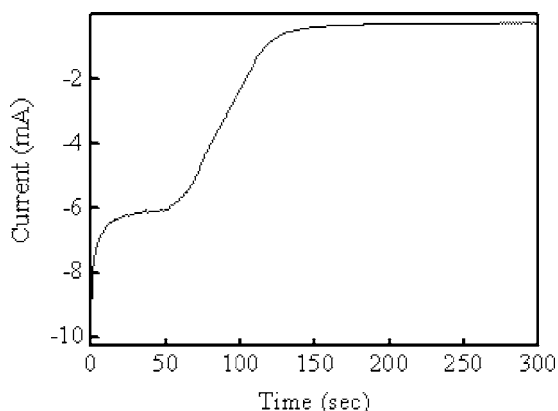


Figure 4. Current-time curves during the anodic dealloying of copper samples that have been electrodeposited with 6.35 C cm⁻² of zinc and anodically dealloyed at 0.4 V. The temperature was 120°C.

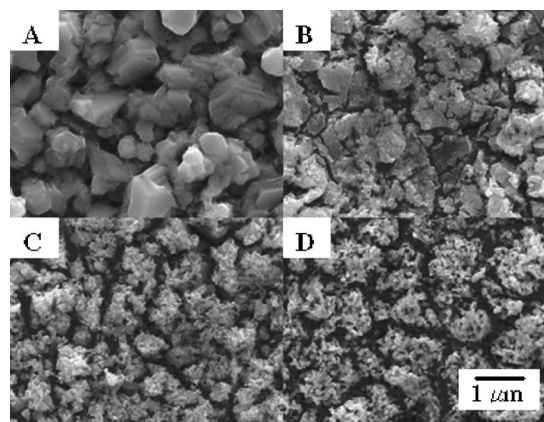


Figure 5. Plan-view SEM images of copper wire samples that have been electrodeposited at 120°C with 2.54 C cm⁻² of zinc followed by dealloying at 0.4 V. The amount (in C cm⁻²) of the zinc that was dealloyed is (A) 1.27 C cm⁻², (B) 1.59 C cm⁻², (C) 1.91 C cm⁻², and (D) 2.54 C cm⁻². The dealloying temperature was 120°C.

difference is not known, but may be the result from the relative differences in the rates of the alloy phase transformation and diffusion of the metal atoms.

The evolution of the porous copper surface during dealloying is illustrated by the SEM microstructural images shown in Fig. 5. Shown in Fig. 5A is the as-deposited surface which contains the Zn-Cu alloy grains. As the dealloying process started, zinc atoms were selectively removed from the outermost alloy surface, leading to the formation of tiny pits. It appeared that the removal of Zn from the alloy occurs preferentially at the grain boundaries than from other areas, and as a result, during the early stage of the dealloying, the grains turned into islands having tiny pits on them and separated by crevices between them (Fig. 5B). As the dealloying proceeded, the selective dissolution of Zn atoms released more copper atoms onto the surface. The surface diffusion of these copper atoms results in larger ligaments and increased pore size (Fig. 5C). Finally, the grains turned into separated porous Cu islands of aggregated ligaments (Fig. 5D).

The bicontinuous porous Cu structure obtained in this study is similar to those obtained for Au¹⁸ and Ag¹⁹ but different from that obtained for Pt¹⁷ in the previous studies using the same alloying/dealloying approach. For Pt, nano and micro-sized cracks rather than pores were produced after dealloying. Such differences may be a result of the very high melting point and thus, very low surface diffusivity of Pt compared to that of the other three metals.²³

Effect of dealloying potential.—The cyclic voltammogram shown in Fig. 1 shows multiple anodic stripping waves due to the various Cu-Zn alloys. To determine the proper potential for the dealloying of Zn from the Cu-Zn surface alloy, constant potential electrolysis experiments on electrochemically formed Cu-Zn samples were conducted at different dealloying potentials covering the range between 0.05 and 0.40 V. In each experiment, the dealloying electrolysis was continued until the dealloying current decreased to the background value. It was found that consistent with the cyclic voltammogram shown in Fig. 1, when the dealloying potential was less positive than 0.1 V, the dealloying current was fairly low. When the dealloying potential was increased to values more positive than 0.2 V, the dealloying rate (current) increased and the time for completing the dealloying decreased significantly. The dealloying potential not only determines the dealloying rate but also determines the amount of Zn that could be dealloyed from the Cu-Zn alloy. The amount of the Zn dealloyed from the samples at each dealloying potential was estimated from the number of charge passed during the dealloying. By comparing the total amount of the deposited Zn and the amount of the dealloyed Zn, the percentage of

Table I. The percentage of zinc remaining in CuZn samples after dealloying at different potentials.

Dealloying potential (V)	Percentage remaining zinc (%)
0.05	52
0.10	41
0.15	14
0.20	11
0.25	4
0.30	3
0.35	3

the Zn remaining in the Cu–Zn alloy was calculated and presented in Table I. Table I indicates, as can be expected from the XRD patterns shown in Fig. 3, that at less positive dealloying potential, the percentage of the Zn remaining in the alloy is high because only the Cu–Zn alloys with Zn content no less than γ -CuZn could be dealloyed, leading to the β' -CuZn and α -Cu–Zn that require more positive potentials to dealloy. The amount of Zn that remained in the alloy decreased with increasing dealloying potential, and a potential more positive than 0.35 V is required to bring the Zn content to a substantial low level. Shown in Fig. 6 are the plan-view SEM images of these samples. This figure shows that not only a porous Cu

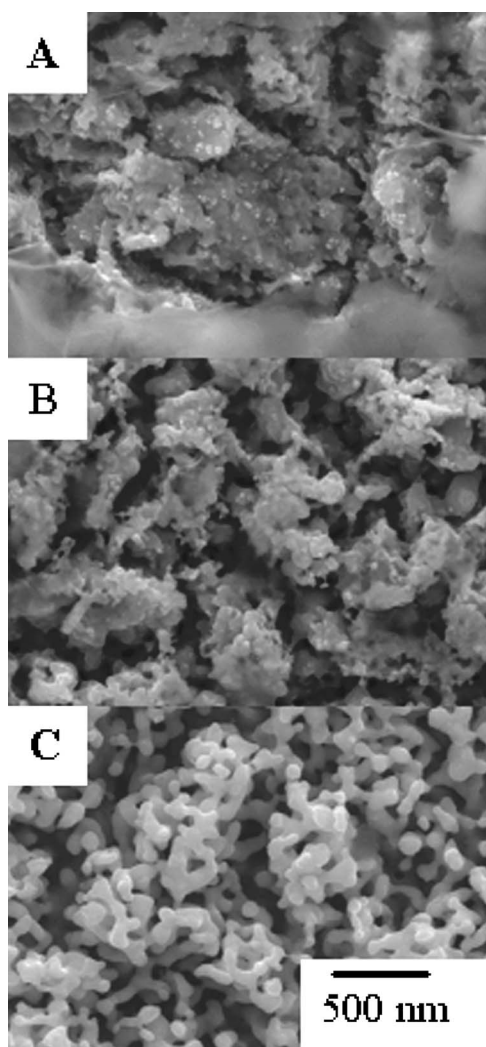


Figure 6. Plan-view SEM images of copper samples that have been electrodeposited with 2.54 C cm^{-2} of zinc with a constant current density of 0.64 mA cm^{-2} at 120°C , and dealloyed at (A) 0.1, (B) 0.2, and (C) 0.35 V.

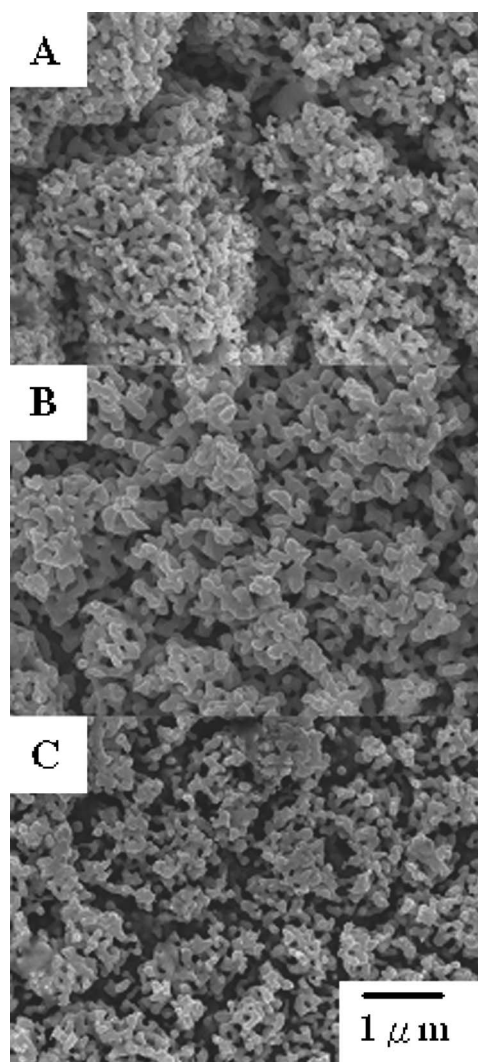


Figure 7. Plan-view SEM images of the porous copper samples prepared by electrodeposition of (A) 6.36 , (B) 3.17 , and (C) 1.59 C cm^{-2} of zinc and anodically dealloyed at 0.40 V . The temperature was 120°C .

surface could be prepared but also a porous Cu–Zn surface could be prepared. As the dealloying potential became more positive, more of the Zn was stripped from the Cu–Zn film, and the coral-like structure of the sample evolved more evidently. It should be mentioned that if the dealloying potential was so positive ($>0.50 \text{ V}$) that dissolution of Cu may occur, the porous structure may be destroyed. For the subsequent experiments, a dealloying potential of 0.40 V was employed.

Effect of deposited zinc quantity.—The amount of zinc that is electrodeposited at the copper surface may affect the composition of the alloy and thus the microstructure of the porous Cu produced after dealloying. A series of porous copper wires was prepared at 120°C by constant current (current density 0.64 mA/cm^2) electrodeposition of different amounts of Zn onto the copper substrate and followed by selective dealloying at a constant potential of 0.40 V . It was found that because increasing the amounts of the deposited Zn resulted in thicker alloy layers, the time period for complete stripping of the Zn from the alloy increased accordingly. The plan-view SEM images of the porous copper wires obtained from the above experiments are shown in Fig. 7. As can be seen from these images, all these samples exhibit coral-like structures formed by aggregated ligament islands. While the ligaments in these samples are of similar sizes, the ligaments' aggregated islands are of

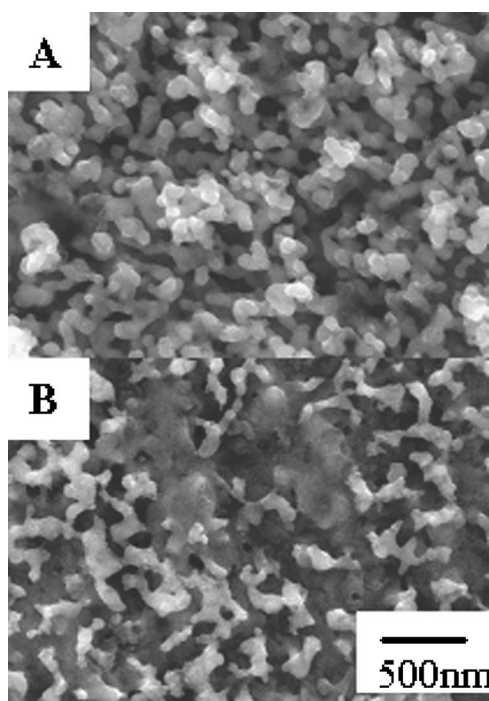


Figure 8. Plain-view SEM images of the copper samples that have been electrodeposited with 2.54 C cm^{-2} of Zn at a constant density (mA cm^{-2}) of (A) 0.4 mA and (B) 1.6 mA, and completely dealloyed at 0.40 V. The temperature was 120°C .

different sizes depending on the quantity of the deposited Zn; alloys having higher Zn content resulted in larger ligament aggregated islands. This phenomenon may be related to the fact that the different charges passed during the deposition step produced deposits of different grain sizes and each grain turned into a ligament aggregate after dealloying. Because increasing the charge for deposition of Zn increases the deposited grain size, larger ligament aggregates were produced after dealloying. It may be worthy to note that the presence of wide crevices between the ligament aggregates could be advantageous for applications in which diffusion of reactants to the deeper layers of the porous material is important.

Effect of zinc deposition current.—The Zn deposition rate (deposition current) may affect the electrodeposited morphology, the time period required for completing the electrodeposition, and the extent of the Cu–Zn alloy formation which in turn may affect the structure of the porous Cu that was produced after dealloying.

Figure 8 shows the plan-view SEM images of the porous Cu after dealloying the Cu–Zn surface alloys that were prepared by electrodeposition of the same amounts of Zn (2.54 C/cm^2) with different deposition currents. It can be seen that a more uniform porous structure was obtained when the Cu–Zn surface alloy was prepared with a lower deposition current (Fig. 8A). This is because at the lower deposition current the deposited Zn is more compact. When the deposition current was high, the deposits became less compact and dealloying of such Cu–Zn film resulted in coarser porous Cu (Fig. 8B).

Effect of dealloying temperature.—The effect of the dealloying temperature on the porous structure was investigated by electrodeposition of zinc on copper wires at a current density of 0.64 mA cm^{-2} at 120°C , and followed by dealloying the formed Ag–Zn film at 0.40 V at 90, 120, and 150°C , respectively. The corresponding SEM images of these samples are shown in Fig. 9. These SEM images show that the pore size and the ligament size both increased with increasing dealloying temperature. This may be

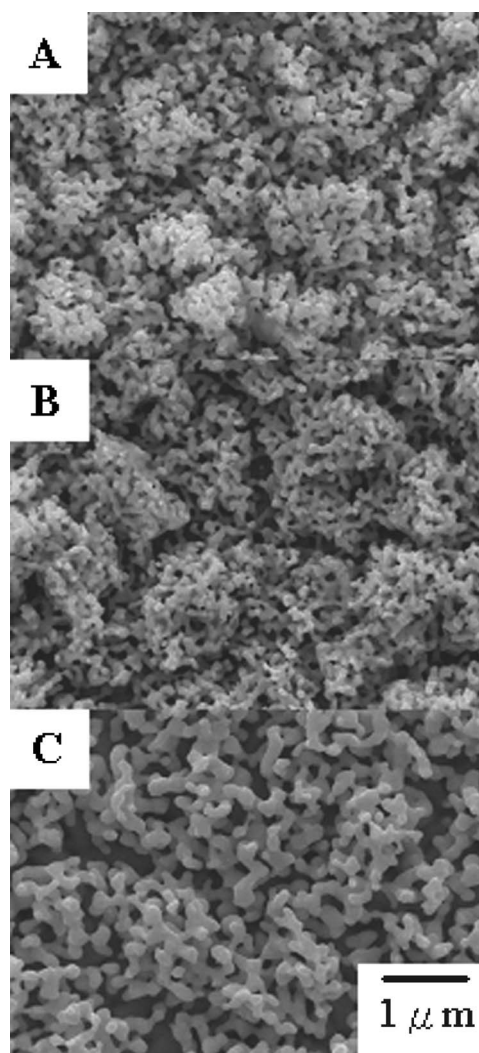


Figure 9. Plan-view SEM images of the copper samples that have been electrodeposited with 2.54 C cm^{-2} of zinc at 120°C and dealloyed at 0.40 V. The dealloying temperature was: (A) 90, (B) 120, and (C) 150°C .

due to the increased surface diffusion rate of the Zn and Cu atoms at higher temperature, which increased the rearrangement and coarsening rate of the Cu porous structure

Conclusion

The preparation of porous copper by electrochemical alloying and dealloying of Cu–Zn alloy from the ZnCl_2 -EMIC ionic liquid was studied. The formation of Cu–Zn alloy by electrodeposition was indicated by cyclic voltammetry, cross-sectional SEM, and XRD measurements. Phase transformation during different stages of dealloying was revealed by XRD measurements. The current-time behavior during the dealloying of the Cu–Zn system was different from that of the Ag–Zn system. While the porous structure produced for the Cu in this study is similar to those obtained for Au and Ag in previous studies, it is different from that for Pt using the same alloying/dealloying approach. The morphologies of the dealloyed material also depend on the dealloying temperature; higher dealloying temperature results in larger pore size due to the increased surface diffusion rate of the metal atoms. The applications of the porous Cu will be studied further.

Acknowledgment

This work was supported by the National Science Council of the Republic of China, Taiwan.

National Cheng-Kung University assisted in meeting the publication costs of this article.

References

1. J. B. Friedrich, M. S. Wainwright, and D. J. Young, *J. Catal.*, **80**, 1 (1983).
2. A. J. Smith, T. Tran, and M. S. Wainwright, *J. Appl. Electrochem.*, **29**, 1085 (1999).
3. J. Toyir, M. Saito, I. Yamauchi, S. C. Luo, J. G. Wu, I. Takahara, and M. Takeuchi, *Catal. Today*, **45**, 245 (1998).
4. A. J. Forty, *Nature (London)*, **282**, 597 (1979).
5. J. D. Fritz and H. W. Pickering, *J. Electrochem. Soc.*, **138**, 3209 (1991).
6. T. P. Moffat, F. R. F. Fan, and A. J. Bard, *J. Electrochem. Soc.*, **138**, 3224 (1991).
7. R. C. Newman, S. G. Corcoran, J. Erlebacher, M. J. Aziz, and K. Sieradzki, *MRS Bull.*, **24**, 24 (1999).
8. J. Erlebacher, M. J. Aziz, A. Karma, N. Dimitrov, and K. Sieradzki, *Nature (London)*, **410**, 450 (2001).
9. Y. Ding, Y. J. Kim, and J. Erlebacher, *Adv. Mater. (Weinheim, Ger.)*, **16**, 1897 (2004); J. Erlebacher, *J. Electrochem. Soc.*, **151**, C614 (2005).
10. H. W. Pickering and C. J. Wang, *J. Electroanal. Chem. Interfacial Electrochem.*, **114**, 698 (1967).
11. M. J. Pryor and J. C. Fister, *J. Electrochem. Soc.*, **131**, 1230 (1984).
12. D. V. Pugh, A. Dursun, and S. G. Corcoran, *J. Mater. Res.*, **18**, 216 (2003).
13. S. I. Hsiu, J. F. Huang, I. W. Sun, C. H. Yuan, and J. Shiea, *Electrochim. Acta*, **47**, 4367 (2002).
14. P. Y. Chen and I. W. Sun, *Electrochim. Acta*, **46**, 1169 (2001).
15. J. F. Huang and I. W. Sun, *J. Electrochem. Soc.*, **149**, E348 (2002).
16. M. C. Lin, P. Y. Chen, and I. W. Sun, *J. Electrochem. Soc.*, **148**, C653 (2001).
17. J. F. Huang and I. W. Sun, *Chem. Mater.*, **16**, 1829 (2004).
18. J. F. Huang and I. W. Sun, *Adv. Funct. Mater.*, **15**, 989 (2005).
19. F. H. Yeh, C. C. Tai, J. F. Huang, and I. W. Sun, *J. Phys. Chem. B*, **110**, 5215 (2006).
20. J. S. Wilkes, J. A. Levisky, and R. A. Wilson, *Inorg. Chem.*, **21**, 1263 (1982).
21. H. Baker, *Alloy Phase Diagrams*, ASM International, Materials Park, OH (2006).
22. A. Katagiri and M. Nakata, *J. Electrochem. Soc.*, **150**, C585 (2003); T. Fukumizu, F. Kotani, A. Yoshida, and A. Katagiri, *J. Electrochem. Soc.*, **153**, C629 (2006).
23. E. G. Seebauer and C. E. Allen, *Prog. Surf. Sci.*, **49**, 265 (1995).